Differential Modulation Diversity for OFDM

Lutz H.-J. Lampe
Laboratorium für Nachrichtentechnik
Universität Erlangen–Nürnberg, Germany
Email: LLampe@LNT.de

Robert Schober
Department of Electrical and Computer Engineering
University of Toronto, Canada
Email: rschober@comm.utoronto.ca

Abstract— **The application of differential modulation diversity (DMD) to orthogonal frequency division multiplexing with multiple transmit and/or receive antennas is considered. Based on diagonal signals originally designed for differential space-time modulation, DMD is used to exploit both space and frequency diversity. At the receiver, low-complexity decision-feedback differential detection without channel state information is employed. Judging from analytical expressions for the pairwise error probability, the improvements and effects due to spatial and/or spectral modulation diversity are pointed out. The numerical results are in good accordance with the presented simulation results.**

I. INTRODUCTION

Orthogonal frequency division multiplexing (OFDM) is an attractive technique for transmission over frequency-selective channels since it allows for low-complexity channel equalization at the receiver [1]. More specifically, OFDM decomposes the frequency-selective channel into orthogonal non-frequency-selective subchannels with complex fading gains equal to the samples of the underlying channel transfer function. However, as the channel transfer function may considerably vary over the frequency range used for transmission, unequal detection error probabilities for different OFDM subchannels result. In particular, the average error probability is dominated by the worst-case error rate. To overcome this limitation[1], some kind of diversity has to be utilized in the detection process.

For this purpose, differential modulation diversity (DMD) recently introduced for transmission over flat fading channels [2] is adapted to OFDM. Although DMD, in general, can exploit time, frequency, and space diversity, here we focus on frequency and space diversity to keep the transmission delay low. Space diversity refers to an increased number of transmit (N_T) and/or receive (N_R) antennas. In contrast to previous approaches [3], [4], where coherent OFDM transmission is regarded, DMD enables noncoherent reception without channel state information (CSI) at the receiver. This is particularly appealing as channel estimation units, possibly for a number of communication links if $N_T > 1$ and/or $N_R > 1$, are not required.

[1] We assume that no channel information is available at the transmitter, i.e., bit- and/or power loading is not possible.

The proposed diversity scheme is based on diagonal signals originally designed for differential space-time modulation (DSTM) over block flat fading channels [5], [6]. At the receiver, low-complexity yet power-efficient decision-feedback differential detection (DF-DD) presented for DSTM in [7] is adopted.

To assess the system performance, expressions for the pairwise error probability and an approximation for the bit error rate (BER) for DF-DD are derived. Both numerical and simulation results for typical mobile communication scenarios confirm in good accordance the efficiency of DMD for noncoherent OFDM transmission. Although we mainly focus on uncoded transmission, we would like to mention that DMD can be straightforwardly combined with error-correction coding.

II. PRELIMINARIES

In this section, the frequency-selective fading channel model and OFDM transmission are discussed, and diagonal signals are briefly reviewed. First, some notation is set.

Notation

Bold upper case $\boldsymbol{X}$ and lower case $\boldsymbol{x}$ denote matrices and vectors, respectively. $\det(\cdot)$, $(\cdot)^T$, $(\cdot)^H$, and $(\cdot)^*$ refer to the determinant of a matrix, transposition, Hermitian transposition, and complex conjugation, respectively. $\mathrm{diag}\{x_1, x_2, \ldots, x_L\}$ is a diagonal matrix with main diagonal elements $x_1, x_2, \ldots, x_L$, whereas $\boldsymbol{I}_M$ and $\boldsymbol{0}_M$ are the $M \times M$ identity matrix and the $M \times M$ all-zero matrix, respectively. $\Pr\{\cdot\}$, $\mathrm{E}\{\cdot\}$, $\mathrm{Re}\{\cdot\}$, and $\otimes$ denote the probability of the event in brackets, expectation, the real part of a complex number, and the Kronecker product, respectively. Throughout this paper, all signals are represented by their complex-baseband equivalents.

Frequency-Selective Fading Channel Model

We consider OFDM for a mobile communications scenario using N_T transmit and N_R receive antennas. The continuous-time multipath channel between the μth transmit and νth receive antenna is described by the input delay-spread function [8]

$$h_{\mu\nu}(\tau,t) = \sum_{i=0}^{L_h-1} h^i_{\mu\nu}(t) g(\tau-\tau_i) \ , \qquad (1)$$

where L_h is the number of propagation paths, τ_i denotes the delay of the ith path, $h^i_{\mu\nu}(t)$ represents the corresponding complex amplitude, and $g(t)$ includes the effects of transmit and receive filter. Assuming the widely applied Gaussian wide-sense stationary uncorrelated scattering (GWSSUS) channel, $h^i_{\mu\nu}(t)$ are mutually uncorrelated WSS zero-mean complex Gaussian processes with variances σ_i^2 and identical normalized time covariance functions. The functions $h_{\mu\nu}(\tau,t)$ of different antenna pairs are presumed as mutually independent with identical channel profile, i.e., L_h and τ_i and time correlation of $h^i_{\mu\nu}(t)$ are the same.

For OFDM transmission the time-variant channel transfer function $H_{\mu\nu}(f,t)$, which is the Fourier transform of $h_{\mu\nu}(\tau,t)$ with respect to τ, is important. With $G(f)$ as Fourier transform of $g(t)$, from (1) we have

$$H_{\mu\nu}(f,t) = G(f) \left(\sum_{i=0}^{L_h-1} h^i_{\mu\nu}(t) \mathrm{e}^{-\mathrm{j}2\pi f \tau_i} \right) \ . \qquad (2)$$

Usually, $|G(f)| \approx 1$ is true in the frequency range of interest and thus, the particular choice of $G(f)$ can be neglected. Applying Clarke's model [9] with maximum Doppler frequency f_D, the random process $H_{\mu\nu}(f,t)$ is described by its covariance function [10] ($\mathrm{J}_0(\cdot)$: zeroth order Bessel function of the first kind)

$$\begin{aligned} \psi_{HH}(f',t') &\triangleq \mathrm{E}\{H_{\mu\nu}(f+f',t+t')H^*_{\mu\nu}(f,t)\} \\ &= \mathrm{J}_0(2\pi f_D t') \sum_{i=0}^{L_h-1} \sigma_i^2 \mathrm{e}^{-\mathrm{j}2\pi f' \tau_i} \ . \qquad (3) \end{aligned}$$

OFDM Transmission

OFDM with D subcarriers spectrally spaced by Δf and guard interval $D_g \cdot T$ (T: modulation interval) is applied. Assuming proper dimensioning of D and D_g such that the transmission channel remains almost constant during one OFDM block of length $T_f = (D + D_g)T$ and interblock interference is practically avoided, the coefficient

$$H_{\mu\nu}[m,k] \triangleq H_{\mu\nu}(m\Delta f, kT_f) \ , \qquad (4)$$

$0 \le m \le D-1$, $k \in \mathbb{Z}$, represents the effective flat fading channel for the mth subcarrier of the kth OFDM block, cf. e.g. [11].

Furthermore, the discrete-time received signal at subcarrier m and antenna ν is impaired by a complex additive white Gaussian noise (AWGN) process $n_\nu[m,k]$. The AWGN processes are presumed to be spatially, temporally, and spectrally uncorrelated and to have equal variance $\sigma_n^2 = \mathcal{E}\{|n_\nu[m,k]|^2\}$, $0 \le \nu \le N_R - 1$.

Diagonal Signals

The concept of DMD is based on diagonal signals introduced in [5], [6]. The diagonal matrix $\boldsymbol{V}[m,k] = (\boldsymbol{V}_1)^{l[m,k]}$ taken from the set $\mathcal{V} = \{\boldsymbol{V}_l = \mathrm{diag}\{\exp(\mathrm{j}2\pi u_0 l/L), \ \ldots, \exp(\mathrm{j}2\pi u_{N_S-1} l/L)\} | l \in \{0, 1 \ldots, L-1\}\}$ of size $L = 2^{N_S R}$ is addressed by the data symbol $l[m,k]$, where $m,k \in \mathbb{Z}$ represent discrete-frequency and discrete-time index, respectively. The data rate is R bits per channel use. Then, N_S jointly modulated transmitted symbols $s_\eta[m,k]$, $0 \le \eta \le N_S - 1$, arranged in the diagonal matrix $\boldsymbol{S}[m,k] \triangleq \mathrm{diag}\{s_0[m,k] \ \ldots, \ s_{N_S-1}[m,k]\}$ are obtained by differential encoding. Applying DMD to OFDM, differential encoding can be done in frequency direction

$$\boldsymbol{S}[m,k] = \boldsymbol{V}[m,k]\boldsymbol{S}[m-1,k] \qquad (5)$$

or in time-direction

$$\boldsymbol{S}[m,k] = \boldsymbol{V}[m,k]\boldsymbol{S}[m,k-1] \ . \qquad (6)$$

For optimum power efficiency, the coefficients u_η, $0 \le \eta \le N_S - 1$, have to be optimized to maximize the diversity product [6]. For the numerical results presented in Section VI, the parameters given in [6, Table I] are adopted.

III. Differential Modulation Diversity for OFDM

In this section, diagonal signals, originally proposed to utilize space diversity only [5], [6], are applied to OFDM to exploit jointly space and frequency diversity.

We distinguish two possible scenarios for OFDM transmission. Whereas for single-block transmission OFDM symbols consecutive in time are supposed to be transmitted independently of each other, for multiple-block transmission one communication link is established over a number of OFDM blocks.

Single-Block Transmission

In case of single-block transmission differential encoding has to be performed across subcarriers, i.e., in frequency direction (5).

To exploit both space and frequency diversity, $N_S = N_B N_T$ (scalar) symbols are jointly modulated and the corresponding matrix symbol is transmitted over N_T antennas and N_B subcarriers for each antenna. This

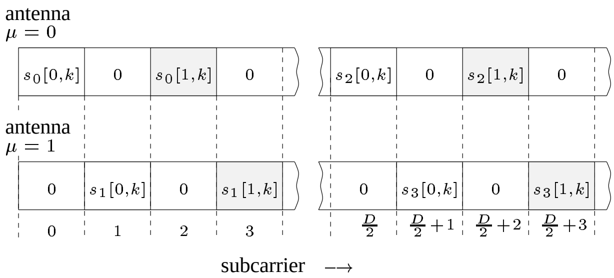

Fig. 1. Differential modulation diversity for OFDM transmission and $N_T = 2$, $N_B = 2$.

means, $N_I \triangleq D/N_S = D/(N_B N_T)$ matrix symbols[2] $\boldsymbol{S}[m,k] = \mathrm{diag}\{s_0[m,k] \ldots s_{N_T N_B - 1}[m,k]\}$, $0 \le m \le N_I - 1$, are transmitted within one OFDM block. For low correlation with respect to frequency, it is convenient to choose the N_B subcarriers to be spectrally spaced by $N_I N_T \Delta f$.

Formally, we write N_I subsequent matrix symbols $\boldsymbol{S}[m,k]$ in the vector $\boldsymbol{s}[k] \triangleq [s_0[0,k]\ s_1[0,k] \ldots s_{N_T N_B-1}[0,k]\ s_0[1,k] \ldots s_{N_T N_B-1}[N_I-1,k]]$ of $D = N_T N_B N_I$ transmit symbols. This vector is partitioned into N_T subblocks $\boldsymbol{s}_\mu \triangleq [s_\mu[0,k]\ s_{N_T+\mu}[0,k] \ldots s_{N_T(N_B-1)+\mu}[0,k]\ s_\mu[1,k] \ldots s_{N_T(N_B-1)+\mu}[N_I - 1,k]]$, $0 \le \mu \le N_T - 1$, of length $N_B N_I$, each associated with one transmit antenna. Specifically, at frequency $N_T N_I \kappa + N_T m + \mu$, $0 \le \mu \le N_T - 1$, $0 \le \kappa \le N_B - 1$, $0 \le m \le N_I - 1$, antenna μ transmits the symbol $s_{N_T\kappa+\mu}[m,k]$, while the remaining $N_T - 1$ antennas are not active. For the example of $N_T = 2$ and $N_B = 2$ the modulation scheme is illustrated in Fig. 1.

At receive antenna ν the D received samples $r_\nu[w,k]$, $w \triangleq N_T N_B m + N_T\kappa + \mu$, are arranged such that $N_T N_B$ successive symbols correspond to one matrix symbol $\boldsymbol{S}[m,k]$

$$r_\nu[w,k] = H_{\mu\nu}[w',k] s_{N_T\kappa+\mu}[m,k] + n_\nu[w',k]\ , \quad (7)$$

$w' \triangleq N_T N_I \kappa + N_T m + \mu$, $0 \le \mu \le N_T - 1$, $0 \le \kappa \le N_B - 1$, $0 \le m \le N_I - 1$.

Multiple-Block Transmission

For the scenario of multiple-block transmission we concentrate on differential encoding in time direction (6). This is motivated by the fact that usually the channel coefficients $H[m,k]$ are stronger correlated in time (k) than in frequency (m) since OFDM requires the channel to be virtually time-invariant during the block duration T_f. Furthermore, we restrict DMD to utilize space and/or frequency diversity. Although, in general, DMD with diagonal signals is qualified for exploiting jointly space, frequency, and time diversity, the latter would entail large transmission delays.

Then, as for single-block transmission, N_I matrix symbols $\boldsymbol{S}[m,k]$, $0 \le m \le N_I - 1$, are transmitted within one OFDM block at time k (see Fig. 1), but differential encoding is performed with respect to k (6). Consequently, the input-output relation (7) remains valid also for multiple-block transmission, but the noncoherent receiver processing differs as explained subsequently.

IV. Decision-Feedback Differential Detection

For power-efficient yet low-complexity noncoherent multiple-antenna transmission without CSI, DF-DD as devised in [7] for the flat fading case can be favorably applied to the current situation.

For DF-DD and differential encoding in time (frequency) $N-2$ previously decided symbols $\hat{l}[m,k-\xi]$ ($\hat{l}[m-\xi,k]$), $1 \le \xi \le N-2$, are employed to decide on $l[m,k]$. In perfect analogy to the flat fading case [7], [2] the DF-DD decision rule reads

$$\hat{l}[m,k] = \underset{l}{\mathrm{argmax}} \Big\{ \mathrm{Re}\Big\{ \sum_{\mu=0}^{N_T-1} \sum_{\kappa=0}^{N_B-1} \sum_{\nu=0}^{N_R-1} \exp\left(\mathrm{j}\frac{2\pi u_{N_T\kappa+\mu} l}{L}\right) \cdot r_\nu^*[N_T N_B m + N_T\kappa + \mu, k] \cdot \hat{r}^{t/f}_{\mathrm{ref},\nu} \Big\}\Big\} \quad (8)$$

with the reference signal $\hat{r}^t_{\mathrm{ref},\nu}$ for differential encoding in time

$$\begin{aligned} \hat{r}^t_{\mathrm{ref},\nu} &= \hat{r}^t_{\mathrm{ref},\nu}[N_T N_B m + N_T\kappa + \mu, k-1] \\ &\triangleq \sum_{\xi=1}^{N-1} p^t_\xi \prod_{n=1}^{\xi-1} \exp\left(\mathrm{j}\frac{2\pi u_{N_T\kappa+\mu}\hat{l}[m,k-n]}{L}\right) \\ &\quad \cdot r_\nu[N_T N_B m + N_T\kappa + \mu, (k-\xi)] \end{aligned} \quad (9)$$

and the reference signal $\hat{r}^f_{\mathrm{ref},\nu}$ for differential encoding in frequency

$$\begin{aligned} \hat{r}^f_{\mathrm{ref},\nu} &= \hat{r}^f_{\mathrm{ref},\nu}[N_T N_B (m-1) + N_T\kappa + \mu, k] \\ &\triangleq \sum_{\xi=1}^{N-1} p^f_\xi \prod_{n=1}^{\xi-1} \exp\left(\mathrm{j}\frac{2\pi u_{N_T\kappa+\mu}\hat{l}[m-n,k]}{L}\right) \\ &\quad \cdot r_\nu[N_T N_B (m-\xi) + N_T\kappa + \mu, k]\ , \end{aligned} \quad (10)$$

respectively. Here, p^t_ξ and p^f_ξ, $1 \le \xi \le N-1$, are the coefficients of an $(N-1)$st order linear predictor for the process

$$c^t_{\mu\nu}[m,k] \triangleq H_{\mu\nu}[m,k] + n_\nu[m,k], \quad (11)$$

with respect to k and

$$c^f_{\mu\nu}[N_T m,k] \triangleq H_{\mu\nu}[N_T m,k] + n_\nu[N_T m,k], \quad (12)$$

[2] We assume an integer ratio $D/(N_B N_T)$ which can always be accomplished by adjusting the number of active subcarriers.

with respect to m, respectively. The predictor coefficients can be calculated from the *Wiener-Hopf equation* or adaptively by application of the recursive least-squares (RLS) algorithm [12], [7].For $N = 2$ DF-DD is equivalent to conventional DD [6].

V. Performance Analysis

To analyze the performance of DMD for OFDM with DF-DD an expression for the pairwise error probability $P_e(l_1, l_2)$ of detecting $\hat{l}[m,k] = l_2$, when $l[m,k] = l_1$ ($l_1,\ l_2 \in \{0,\ 1,\ \ldots,\ L-1\}$, $l_1 \neq l_2$) is transmitted, is given. Based on $P_e(l_1, l_2)$ the bit-error rate (BER) is approximated. For mathematical tractability we assume perfect feedback, i.e., $\hat{l}[m, k-\xi] = l[m, k-\xi]$ ($\hat{l}[m-\xi, k] = l[m-\xi, k]$) is introduced in (9) ((10)). In general, it turns out that error propagation increases BER by a factor of two and thus, the approximate error rate for realizable DF-DD may be obtained by doubling the error rate for genie-aided DF-DD.

Pairwise Error Probability

For genie-aided DF-DD from (7) and (8) the pairwise error probability can be expressed as [2]

$$P_e(l_1, l_2) = \Pr\{\Delta(l_1, l_2) < 0\} \tag{13}$$

with the Hermitian quadratic form of zero-mean complex Gaussian distributed random variables

$$\Delta(l_1, l_2) = \boldsymbol{g}^H \boldsymbol{F} \boldsymbol{g} \ . \tag{14}$$

Here, the definitions

$$\boldsymbol{F} \triangleq \begin{bmatrix} \boldsymbol{0}_{N_T N_B N_R} & \boldsymbol{C}^H \\ \boldsymbol{C} & \boldsymbol{0}_{N_T N_B N_R} \end{bmatrix} \tag{15}$$

$$\boldsymbol{C} \triangleq \boldsymbol{I}_{N_R} \otimes \mathrm{diag}\left\{C_{00}, C_{10}, \ldots, C_{N_T-1 N_B-1}\right\} \tag{16}$$

$$\boldsymbol{g} \triangleq [\boldsymbol{x}^T \ (\boldsymbol{y}^{t/f})^T]^T \tag{17}$$

$$\boldsymbol{x} \triangleq [x_{00}[m,k,0] \ \ldots \ x_{N_T-10}[m,k,0] \, x_{00}[m,k,1] \ \ldots x_{N_T-1 N_R-1}[m,k,N_B-1]]^T \tag{18}$$

$$\boldsymbol{y}^t \triangleq [y^t_{00}[m,k-1,0] \ \ldots \ y^t_{N_T-10}[m,k-1,0] \ \ldots \ y^t_{N_T-1 N_R-1}[m,k-1,N_B-1]]^T \tag{19}$$

$$\boldsymbol{y}^f \triangleq [y^f_{00}[m-1,k,0] \ \ldots \ y^f_{N_t-10}[m-1,k,0] \ \ldots \ y^f_{N_T-1 N_R-1}[m-1,k,N_B-1]]^T \tag{20}$$

$$C_{\mu\kappa} \triangleq 1 - \exp\left(\mathrm{j}2\pi u_{N_T\kappa+\mu}(l_1 - l_2)/L\right) \tag{21}$$

$$x_{\mu\nu}[m,k,\kappa] \triangleq H_{\mu\nu}[N_T N_I \kappa + N_T m + \mu, k] + n_\nu[N_T N_I \kappa + N_T m + \mu, k] s^*_{N_T\kappa+\mu}[m,k] \tag{22}$$

$$y^t_{\mu\nu}[m,k-1,\kappa] \triangleq \sum_{\xi=1}^{N-1} p^t_\xi x_{\mu\nu}[m,k-\xi,\kappa] \tag{23}$$

$$y^f_{\mu\nu}[m-1,k,\kappa] \triangleq \sum_{\xi=1}^{N-1} p^f_\xi x_{\mu\nu}[m-\xi,k,\kappa] \ . \tag{24}$$

are used, and the superscripts ^{t} and ^{f} refer to differential encoding in time and frequency, respectively.

With the Laplace transform [13]

$$\Phi_{\Delta(l_1,l_2)}(s) = \left(\det\{\boldsymbol{I}_{2N_T N_B N_R} + s\boldsymbol{\Psi}_{gg}\boldsymbol{F}\}\right)^{-1} \tag{25}$$

of the probability density function (pdf) of $\Delta(l_1, l_2)$, where the covariance matrix $\boldsymbol{\Psi}_{gg} \triangleq \mathcal{E}\{\boldsymbol{g}\boldsymbol{g}^H\}$ depends exclusively on $\psi_{HH}(f', t')$, and σ_n^2 defined in Section II, $P_e(l_1, l_2)$ can now be calculated as

$$P_e(l_1, l_2) = \frac{1}{2\pi \mathrm{j}} \int_{\gamma-\mathrm{j}\infty}^{\gamma+\mathrm{j}\infty} \Phi_{\Delta(l_1,l_2)}(s) \, \frac{\mathrm{d}s}{s} \ , \tag{26}$$

where $\gamma > 0$ lies in the region of convergence of $\Phi_{\Delta(l_1,l_2)}(s)$. A closed-form solution for the integral (26) may be obtained by the residue method, cf. [14]. $P_e(l_1, l_2)$ can be also efficiently computed based on a change of variable and Gauss-Chebyshev quadrature rules [15].

Approximation for BER

The results of the previous section may be used to obtain an approximation for BER. Using the group property of diagonal signals [5], [6] and applying Gray labeling for the $N_T N_B R$ bits assigned to the symbols l (i.e., matrix $\boldsymbol{V}_l$), $0 \leq l \leq L-1$, a simple approximation for the BER for genie-aided DF-DD is obtained by [2]

$$P_b^{\text{genie}} \approx \frac{1}{N_T N_B R} \sum_{l=1}^{L-1} P_e(l, 0) \ . \tag{27}$$

For $N > 2$ erroneous feedback symbols increase BER approximately by a factor of two (cf. [2]). Hence, an approximation for the BER of realizable DF-DD is

$$P_b \approx \begin{cases} P_b^{\text{genie}}, & N = 2 \\ 2 \cdot P_b^{\text{genie}}, & N > 2 \end{cases} \ . \tag{28}$$

This result will be used in the next section to support our simulations and to discuss the properties of DMD for OFDM with DF-DD.

VI. Results and Discussion

The channel model described in Section II with typical urban (TU), hilly terrain (HT), and equalizer test (EQ) power delay profiles [16] is used for simulation and analytical performance evaluation of the proposed DMD for OFDM. We adopt the OFDM parameters from

[10], [3], i.e., there are $D = 120$ active subcarriers, subcarrier spacing is $\Delta f = 6250$ Hz, and block duration is $T_f = 200\ \mu$s including a guard time of 40 μs. Focusing on transmit (modulation) diversity, we restrict ourselves to the case of one receive antenna ($N_R = 1$). Diagonal constellations with $R = 2$ bits/(channel use) are employed. As measure of power efficiency we define the signal-to-noise ratio $\mathrm{SNR} = \sum_{i=0}^{L_h-1} \sigma_i^2/\sigma_n^2$.

Single-Block Transmission

First, we consider DMD with pure frequency diversity ($N_T = 1$). Figs. 2a), b), and c) show BER vs. $10\log_{10}(\mathrm{SNR})$ for $N_B = 1$, $N_B = 2$, and $N_B = 3$, respectively, and the TU power delay profile. Apparently, increasing N_B combats the frequency-selective behavior of the transmission channel. In addition, DF-DD with $N = 5$ yields a higher power efficiency than conventional DD ($N = 2$) and in the SNR range of interest an error floor can be avoided. We note that the numerical approximation and the simulation results match remarkably well.

Next, the BER's for DMD with pure space diversity ($N_B = 1$) are depicted in Figs. 3a), b), and c) for $N_T = 1$, $N_T = 2$, and $N_T = 3$, respectively. Again, the TU power delay profile is exemplarily considered. The curves are very similar to the case of pure frequency diversity in Figs. 2a), b), and c) (Figs. 2a) and 3a) show identical curves for $N_T = N_B = 1$). However, whereas idealized coherent transmission with perfect CSI can benefit from the increased spatial diversity compared to the spectral diversity, noncoherent transmission with conventional DD suffers from a high error floor. Although through DF-DD with $N = 5$ this error floor vanishes, the performance gap to coherent reception increases with N_T. This behavior is due to the higher effective fading rate (in frequency direction) of the process $c^f_{\mu\nu}[N_T m, k]$ in (12), which grows with N_T.

To further highlight the influence of space and frequency diversity, different diversity schemes with $N_T \cdot N_B = 4$ are compared for the TU, HT, and EQ channel in Figs. 4a), b), and c), respectively. Approximations of BER are exclusively shown. As for coherent reception with perfect CSI the effective fading rate has no influence on BER, the best performance is always achieved with $N_T = 4$ ($N_B = 1$) spatially uncorrelated transmit antennas. We observe that for the EQ channel frequency diversity is almost as effective as space diversity. On the other hand, for conventional DD $N_B = 4$ ($N_T = 1$) yields the lowest error floor, and the EQ channel constitutes the worst-case scenario. When applying DF-DD with $N = 5$, DMD exploiting frequency and space diversity with $N_B = N_T = 2$ turns out to be robust solution with respect to the different channel scenarios.

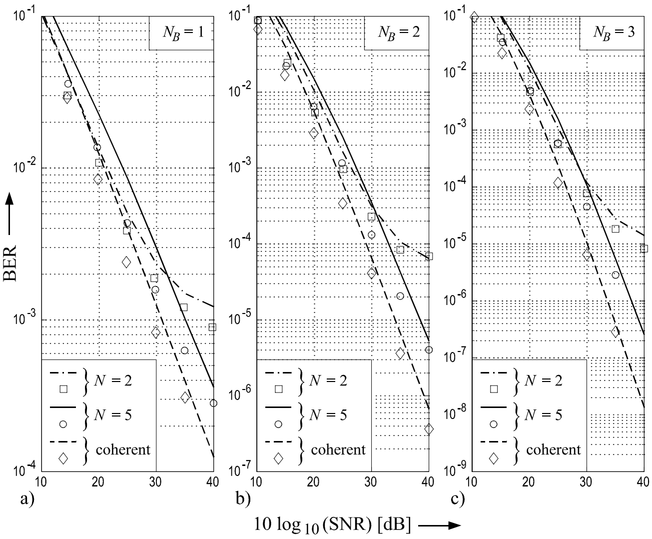

Fig. 2. BER vs. $10\log_{10}(\mathrm{SNR})$ for $N_T = 1$ and a) $N_B = 1$, b) $N_B = 2$, and c) $N_B = 3$. Single-block transmission over TU channel. □, ○, and ◇ denote simulation points.

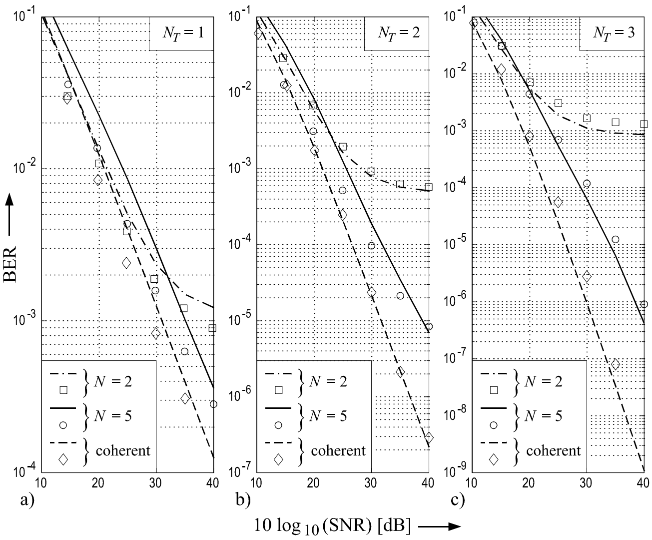

Fig. 3. BER vs. $10\log_{10}(\mathrm{SNR})$ for $N_B = 1$ and a) $N_T = 1$, b) $N_T = 2$, and c) $N_T = 3$. Single-block transmission over TU channel. □, ○, and ◇ denote simulation points.

Clearly, DF-DD bridges the gap between conventional DD and coherent detection.

Multiple-Block Transmission

Since for multiple-block transmission with differential encoding in time direction the number of transmit antennas N_T does not influence the effective fading rate (compare $c^t_{\mu\nu}[m, k]$ and $c^f_{\mu\nu}[N_T m, k]$ in (11) and (12), respectively), increasing N_T is beneficial in all cases. Hence, for the scenario of spatially uncorrelated antenna links considered here, N_T should be chosen as large as possible, i.e., an exchange between N_T and N_B for fixed $N_T \cdot N_B$ (see Fig. (4)) is not recommended.

Assuming a TU channel with maximum Doppler frequency $f_D = 40$ Hz ($f_D T_f = 0.008$), numerical results of BER for a) $N_T = 1$, $N_B = 1$, b) $N_T = 2$,

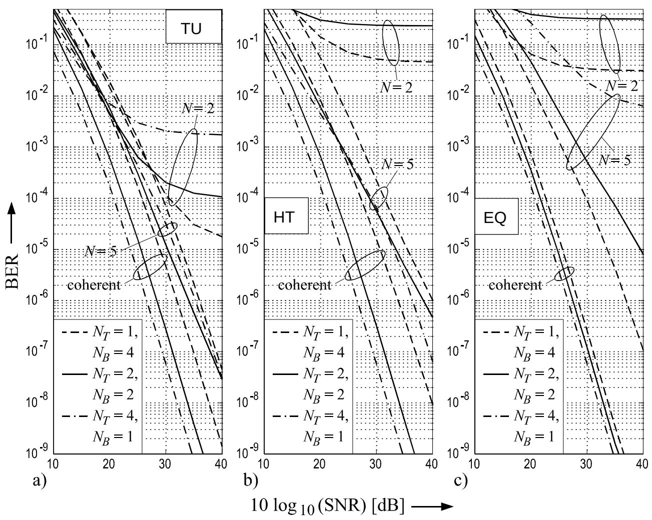

Fig. 4. BER vs. $10\log_{10}(\text{SNR})$ for $N_T \cdot N_B = 4$ and a) TU, b) HT, and c) EQ power delay profile. Single-block transmission. Only numerical results are shown.

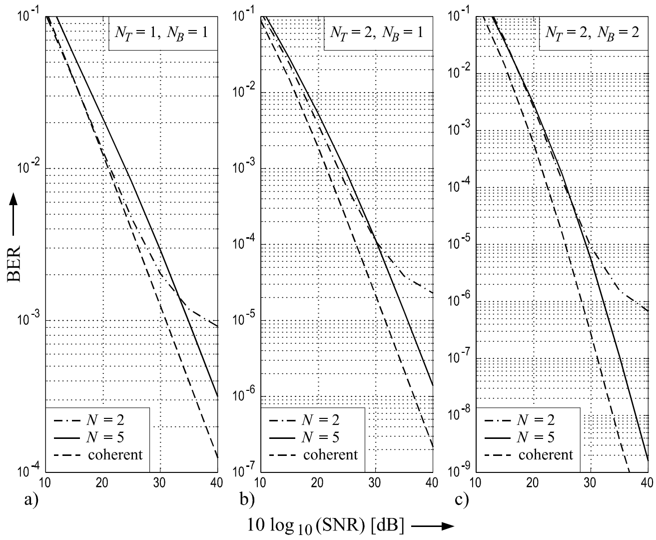

Fig. 5. BER vs. $10\log_{10}(\text{SNR})$ for a) $N_T{=}1, N_B{=}1$, b) $N_T{=}2$, $N_B{=}1$, and c) $N_T{=}2$, $N_B{=}2$. Multiple-block transmission over TU channel. Only numerical results are shown.

$N_B = 1$, and c) $N_T = 2$, $N_B = 2$) are presented in Figs. 5a), b), and c), respectively. Clearly, for $N_B = 1$ (Figs. 5a), b)) space diversity with $N_T = 2$ is a proper means to overcome the limitations by the frequency selective channel. If, additionally, frequency diversity is utilized (Figs. 5c), we assume that only $N_T = 2$ transmit antennas are available) further significant improvements in power efficiency are achieved.

Comparing the results for noncoherent reception and differential encoding in time with the corresponding curves for differential encoding in frequency (Figs. 5a), b) with Figs. 3a), b) and Fig. 5c) with Fig. 4a)), we note that differential encoding in time is advantageous, since for the considered transmission scenario the channel variation in time is smaller than in frequency. Moreover, the gap in power efficieny between coherent reception with perfect CSI and DF-DD with $N = 5$ and the error floor for conventional DD, respectively, do not increase with N_T.

VII. Conclusions

Differential modulation diversity for OFDM is introduced as powerful technique to improve power efficiency for transmission over frequency-selective channels. Both space and frequency diversity are efficiently utilized for OFDM transmission. For noncoherent reception low-complexity DF-DD is favorably applied. The error analysis highlights the effects of space and frequency diversity on the performance of OFDM with differential encoding in time and frequency, respectively. We would like to mention that the application and the performance analysis of DMD can be straightforwardly extented to general spatially correlated frequency-selective Ricean fading channels [2].

References

[1] S.B. Weinstein and P.M. Ebert, "Data Transmission by Frequency-Division Multiplexing Using the Discrete Fourier Transform," *IEEE Com. Mag.*, vol. 19, no. 5, pp. 628–634, Oct. 1971.

[2] R. Schober and L.H.-J. Lampe, "Differential Modulation Diversity," *Submitted to IEEE Transactions on Vehicular Technology*, Feb. 2001.

[3] Y. Li, N. Seshadri, and S. Ariyavisitakul, "Channel Estimation for OFDM Systems with Transmitter Diversity in Mobile Wireless Channels," *IEEE J. Select. Areas Commun.*, vol. 17, no. 3, pp. 461–471, Mar. 1999.

[4] Y. Li, J.C. Chuang, and N.R. Sollenberger, "Transmitter Diversity for OFDM Systems and Its Impact on High-Rate Data Wireless Networks," *IEEE J. Select. Areas Commun.*, vol. 17, no. 7, pp. 1233–1243, July 1999.

[5] B.L. Hughes, "Differential Space-Time Modulation," *IEEE Trans. Inf. Theory*, vol. 46, no. 7, pp. 2567–2578, Nov. 2000.

[6] B.M. Hochwald and W. Sweldens, "Differential Unitary Space-Time Modulation," *IEEE Trans. Com.*, vol. 48, no. 12, pp. 2041–2052, Dec. 2000.

[7] R. Schober and L.H.-J. Lampe, "Noncoherent Receivers for Differential Space-Time Modulation," *In Revision: IEEE Transactions on Communications*, Dec. 2000.

[8] R. Steele, *Mobile Radio Communications*, John Wiley & Sons, Inc., New York, 2nd ed. edition, 1999.

[9] W.C. Jakes, Jr., *Microwave Moble Communications*, John Wiley & Sons, Inc., New York, 1974.

[10] Y. Li, L.J. Cimini, and N.R. Sollenberger, "Robust Channel Estimation for OFDM Systems with Rapid Dispersive Fading Channels," *IEEE Trans. Com.*, vol. 46, no. 7, pp. 902–915, July 1998.

[11] J. Benndorf, D.L. Korobkow, and A.G. Schwanja, "Matched Signals in the Presence of Intersymbol Interference," *AEÜ, Int. Journal of Electronics*, vol. 46, no. 6, pp. 409–414, 1992.

[12] R.J. Young and J.H. Lodge, "Detection of CPM Signals in Fast Rayleigh Flat-Fading Using Adaptive Channel Estimation," *IEEE Trans. Vehicular Technology*, pp. 338–347, May 1995.

[13] M. Schwartz, W. Bennett, and S. Stein, *Communication Systems and Techniques*, McGraw-Hill, New York, 1966.

[14] J.K. Cavers and P. Ho, "Analysis of the Error Performance of Trellis-Coded Modulations in Rayleigh-Fading Channels," *IEEE Trans. Com.*, vol. 40, pp. 74–83, Jan. 1992.

[15] E. Biglieri, G. Caire, G. Taricco, and J. Ventura-Traveset, "Computing Error Probabilities over Fading Channels: A Unified Approach," *Europ. Trans. Telecom. (ETT)*, vol. 9, pp. 15–25, Jan/Feb 1998.

[16] *GSM Recommendation 05.05: "Radio Transmission and Reception", Vers. 8.9.0, Release 1999.*